Carcinogenesis vol.35 no.12 pp.2748–2755, 2014
doi:10.1093/carcin/bgu208
Advance Access publication October 3, 2014

MicroRNA-105 suppresses cell proliferation and inhibits PI3K/AKT signaling in human hepatocellular carcinoma

Gang Shen[†], Xiaoxiang Rong[1,†], Jianbo Zhao[2,†], Xuewei Yang[3], Haibo Li, Hua Jiang, Qiang Zhou[4], Tianxing Ji[4], Sicong Huang[4], Jing Zhang and Hongyun Jia[4,*]

Department of Interventional Radiology and Vascular Anomalies, Guangzhou Women and Children's Medical Center, Guangzhou Medical University, Guangzhou, Guangdong 510623, People's Republic of China, [1]Department of Oncology and [2]Department of Interventional Radiology, Nanfang Hospital, Southern Medical University, Guangzhou, Guangdong 510515, People's Republic of China and [3]Department of Hepatobiliary Surgery and [4]Department of Clinical examination, The Second Affiliated Hospital of Guangzhou Medical University, Guangzhou, Guangdong 510260, People's Republic of China

*To whom correspondence should be addressed. Tel: +86 20 34152548; Fax: +86 20 34152437;
Email: hongyun_jia@163.com
Correspondence may also be addressed to Jing Zhang. Tel: +86 20 81330675; Fax: +86 20 81330666;
Email: fejr@foxmail.com

A growing amount of evidence supports that microRNA (miRNA) dysregulation is involved in cancer progression by directly downregulating multiple targets. Elucidating the underlying mechanism of miRNA in carcinogenesis may improve diagnostic and therapeutic strategies for malignancy. In the current study, we found that miR-105 expression was markedly downregulated in both hepatocellular carcinoma (HCC) cell lines and clinical HCC tissues, compared with normal human hepatocyte and adjacent non-cancerous tissues, respectively. Ectopic miR-105 expression suppressed, whereas inhibiting miR-105 promoted the proliferation and tumorigenicity of HCC cells both *in vitro* and *in vivo*. Furthermore, we demonstrated that miR-105 could deactivated the phosphoinositide 3-kinase (PI3K)/AKT signaling pathway by downregulating insulin receptor substrate-1, 3-phosphoinositide-dependent protein kinase-1 and AKT1 directly, resulting in increasing cyclin-dependent kinase inhibitors 1A and 1B (p21^{Cip1} and p27^{Kip1}) and decreasing cyclin D1 expression in HCC. Therefore, our results suggest that miR-105 functions as a potential tumor suppressor by inhibiting the PI3K/AKT signaling pathway and might represent a potential therapeutic target for HCC patients.

Introduction

Hepatocellular carcinoma (HCC), which accounts for 80–90% of primary liver cancers, is the third most common cause of cancer-related mortality worldwide (1–4). Due to a variety of etiological factors, including hepatitis B and hepatitis C virus infection, aflatoxin-contaminated food and alcohol abuse, the incidence of HCC has increased in the last two decades (1,5). Although surgical hepatic resection and liver transplantation techniques have improved, the overall 5 year survival rate is still only 5% and the long-term prognosis remains dismal (6). Moreover, the precise molecular mechanisms involved in HCC progression are still not completely understood.

Abbreviations: 3′UTR, 3′untranslated region; FOXOs, forkhead transcription factors; GAPDH, glyceraldehyde 3-phosphate dehydrogenase; HCC, hepatocellular carcinoma; IHC, immunohistochemical; IR, insulin receptor; IRS1, insulin receptor substrate-1; miRNA, microRNA; PBS, phosphate-buffered saline; PDK1, 3-phosphoinositide-dependent protein kinase-1; PI3K, phosphoinositide 3-kinase; siRNA, small interfering RNA; Ct, threshold cycle.

[†]These authors contributed equally to this work.

An increasing amount of evidence demonstrates that the therapeutic failure and poor prognosis of HCC are associated with aberrantly activated signaling pathways, such as phosphoinositide 3-kinase (PI3K)/AKT signaling, which has been found to be aberrant activating in HCC and is associated with HCC initiation and progression of HCC (7,8). Excessive AKT activation is a risk factor for early disease recurrence and poor prognosis in HCC and contributes to resistance to first-generation single-agent targeted therapy (9). Additionally, activated AKT signaling results in HCC cell resistance to chemotherapy and radiation and promotes cell survival, whereas inhibiting AKT activation dramatically inhibits the tumorigenicity of HCC (10). Therefore, activation of PI3K/AKT signaling has emerged as a potential target for HCC therapy.

Abnormal activation of PI3K/AKT signaling is associated with dysregulation of pathway component(s), including loss-of-function phosphoinositide phosphatases, such as phosphatase and tensin homolog and PH domain and leucine-rich repeat protein phosphatase 2, and/or gain-of-function elements, such as insulin receptor (IR), IR substrate-1 (IRS1), 3-phosphoinositide-dependent protein kinases (PDKs) and AKT (11–13). An intracellular adapter protein, IRS1, transmits various key extracellular signals such as insulin and insulin-like growth factor to downstream factors, subsequently activating intracellular signaling, including the PI3K/AKT pathway (14,15). Previous studies have suggested that a high degree of IRS1 in human IRS1 transgenic mice was associated with constitutive activation of PI3K signaling cascades and that IRS1 overexpression promotes hepatocyte growth (16). It is well known that PDKs mediate PI3K/AKT signal transduction, and PDK abnormality contributes to the development of many malignancies. PDK1 and PDK2 activate AKT kinase at the locus of Thr308 and Ser473, respectively, and the activated AKT subsequently plays important roles in carcinogenesis and the development, invasion and treatment tolerability of many malignancies, including HCC (17). Abnormal AKT kinase activation contributes to oncogenesis through the regulation of multiple downstream molecules, for instance, increasing the expression of the cell cycle regulator Cyclin D1 and decreasing the expression of forkhead transcription factors (FOXOs) and cyclin-dependent kinase inhibitors 1A and 1B (p21^{Cip1} and p27^{Kip1}) (18,19). Thus, elucidating the molecular mechanism of PI3K/AKT signaling regulation in HCC is both biologically and clinically important for future HCC research and therapy.

MicroRNAs (miRNAs), a class of small, non-coding endogenous RNAs, have been demonstrated to play important regulatory roles in many biological processes. Accumulating reports suggest that miRNAs affect both the tumor initiation and progression processes and may represent as promising targets for tumor diagnosis and therapy (20,21). In the present study, miR-105 was found to repressed HCC proliferation both *in vitro* and *in vivo* by directly targeting the 3′untranslated region (3′UTR) of crucial components of the PI3K/AKT pathway: IRS1, PDK1 and AKT1. Our results suggest that miR-105 downregulation may be important for HCC development and progression, highlighting it as a potential target for HCC therapy.

Materials and methods

Cell culture

The HCC cell lines, Hep3B, MHCC97L, Huh7, HCCC-9810, HepG2, BEL-7402, MHCC97H, QGY-7703 were purchased from the American Type Culture Collection (Manassas, VA) and cultured in Dulbecco's modified Eagle's medium (Invitrogen, Carlsbad, CA) supplemented with 10% fetal bovine serum (Invitrogen), 100 U/ml penicillin and 100 μg/ml streptomycin (Invitrogen). Normal liver epithelial cells LO2 were purchased from the Chinese Academy of Sciences Committee Type Culture Collection cell bank and were cultured under the conditions stated by the manufacturer. Normal liver epithelial cells THLE-3 were purchased from the American Type Culture Collection and cultured as suggested by the manufacturer.

Tissue specimens

This study was conducted on 16 pairs of snap-frozen HCC tumor tissues and matched normal tissues from adjacent regions, which were diagnosed histopathologically at the Second Affilated Hospital of Guangzhou Medical University and the Nanfang Hospital, Southern Medical University, from 2001 to 12. The information of clinical characteristics of all 16 patients, including 1 clinical stage I, 10 clinical stage II, 4 clinical stage III, 1 clinical stage VI. They were immediately stored in liquid nitrogen after surgery until further use. For the use of the clinical materials for research purposes, the Institutional Research Ethics Committee approved the study, and prior patient consent was obtained.

RNA extraction and real-time quantitative PCR

Total miRNA from cultured cells and HCC tissue samples was extracted using the mirVana miRNA Isolation Kit (Ambion, Austin, TX) according to the manufacturer's manual. The expression level of miR-105 was performed using miR-105-specific primer and probe (TaqMan MicroRNA Assay Kit, Applied Biosystems, Foster City, CA) on an ABI 7900 system (Applied Biosystems). The expression of miR-105 was defined based on the threshold cycle (Ct), and relative expression levels were calculated as $2^{-[(\text{Ct of miR-105}) - (\text{Ct of U6})]}$ after normalization with reference to the quantification of *U6* small nuclear RNA expression.

Total cellular RNA was extracted using the TRIzol solution (Invitrogen), according to the manufacturer's protocol. Complementary DNAs were synthesized and real-time PCR was performed using RT Real-Time™ SYBR Green (Bio-Rad Laboratories, Berkeley, CA). Expression levels of genes were normalized to that of the housekeeping gene glyceraldehyde 3-phosphate dehydrogenase (GAPDH) as the control and calculated as $2^{-[(\text{Ct of } \textit{Cyclin D1}, \text{ p21, p27}) - (\text{Ct of } \textit{GAPDH})]}$, where Ct represents the threshold cycle for each transcript. The following primers were used: *Cyclin D1* forward: 5′-AA CTACCTG GACCG C TTCCT-3′; *Cyclin D1* reverse: 5′-CCACTT GAGCTT GTTCACCA-3′; $p21^{Cip1}$ forward: 5′-CGATGCCAA CCTCCTCAACGA -3′; $p21^{Cip1}$ reverse: 5′-TCG CAGA CCT CCAGCATCCA-3′; $p27^{Kip1}$ forward: 5′-TGCAACCGACGATTCTTC TAC TCAA-3′; $p27^{Kip1}$ reverse: 5′-CAAGCAGTGATGTAT CTG ATAAACAAGG A-3′; *GAPDH* forward: 5′-GACTCATGACCACAGTCCATGC-3′; *GAPDH* reverse: 3′-A GAGG CAGGGATGATGTTCTG-5′.

Plasmid, small interfering RNA and transfection

To generate a miR-105 expression vector, approximately 250 bp genomic fragment up and downstream of the pre-miR-105 form was generated by PCR amplification from the genomic DNA of HEK-293 cell and cloned into the XhoI and EcoRI sites of the pMSCV vector (Clontech, Mountain View, CA). The primers for amplifying miR-105 were: miR-105-up: 5′-GCCCTCG AGATA CC AT ATCTATCCCCTTTTTCA-3′; miR-105-dn: 5′-GCCGAATTC CAACCATGA AGAT A CGAATTGATG-3′. The region of the human IRS1 3′UTR, from 2496 to 3137, PDK1 3′UTR, from 865 to 2417, or AKT1 3′UTR, from 51 to 108, was PCR amplified from genomic DNA and cloned into pGL3 luciferase reporter plasmid (Promega, Madison, WI), respectively. Primers were: *PDK1*-3′UTR-up: 5′-GCCAGATCTTAGAGCCTAGAA ATC TCACTTTTTA-3′; *PDK1*-3′UTR-dn: 3′-GCCG TCGACGTCCATTACC ACAATAACAGAGT AA-5′; *IRS1*-3′UTR-up: 5′-GCCAGATC TACCAAAAGTTCATACTCTGGCG ACA-3′; *IRS1*-3′UTR-dn: 3′-GCCCTC GAGGC AAGATTGAATAAAACAGGGCTTC-5′; *AKT1*-3′UTR-up: 5′-GCCAGATCTCTCGTG CCATGATCTGTATTTAATG-3′; *AKT1*-3′UTR-dn: 3′-GCCGT CGACCTGCCCAC AG CACAAAAACGTCTTT-5′; miR-105 mimic oligonucleotides and miR-105 inhibitor (a cholesterol-conjugated 2′-O-Me modified antisense oligonucleotide designed specifically to bind to and inhibit endogenous miR-105 molecule) were synthesized and purified by RiboBio (Guangzhou, Guangdong, China). For depletion of IRS1, PDK1 or AKT1, small interfering RNA (siRNA) was synthesized and purified by RiboBio. The siRNA sequences were used following: IRS1 siRNA: CAGAATGAAGACCTAAATGAC; PDK1 siRNA: CGTG AATATGTTG AAGT AGAA; AKT1 siRNA: GGACAAGGACGGGC ACATTAA; transfection of miRNA, siRNAs and plasmids was performed using the Lipofectamine 2000 reagent (Invitrogen) according to the manufacturer's instruction.

Luciferase assay

Cells were seeded in triplicate in 24-well plate and allowed to settle for 24 h. One hundred nanograms of pGL3-*IRS1*-luciferase plasmid, pGL3-*PDK1*-luciferase plasmid or pGL3-*AKT1*-luciferase plasmid, plus 5 ng of pRL-TK renilla plasmid (Promega) were transfected into HCC cells using the Lipofectamine 2000 reagent (Invitrogen), respectively, according to the manufacturer's instruction. Luciferase and control signals were measured at 48 h after transfection using the Dual Luciferase Reporter Assay Kit (Promega), according to a protocol provided by the manufacturer. Three independent experiments were performed and the data were presented as the mean ± SD.

Western blotting

Cellular proteins were prepared in sample buffer [62.5 mM Tris–HCl (pH 6.8), 10% glycerol, 2% sodium dodecyl sulfate] and heated for 10 min at 100°C. Equal quantities of protein were electrophoresed through a 10% sodium dodecyl sulfate/polyacrylamide gel and transferred to a polyvinylidene difluoride membrane (Millipore, Billerica, MA). The membranes were incubated with anti-IRS1, anti-PDK1, anti-AKT1, anti-FOXO3a, anti-p-FOXO3a, anti-Cyclin D1, anti-p21, anti-p27 (Cell Signaling Technology, Danvers, MA) and anti-Rb, anti-p-Rb antibodies (Abcam, Cambridge, MA), respectively. The membranes were stripped and reblotted with an

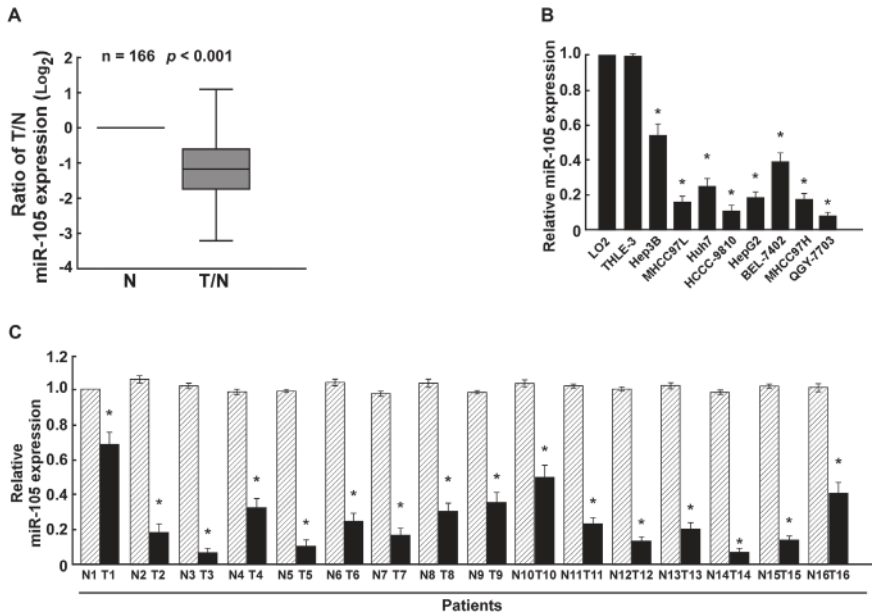

Fig. 1. miR-105 is downregulated in HCC cell lines and tissues. (**A**) Expression profiling of miRNAs showing that miR-105 is downregulated in HCC tissues (T) compared with matched adjacent normal tissue (ANT) (n = 166; NCBI/GEO/GSE31384). (**B**) Real-time PCR analysis of miR-105 expression in normal liver epithelial cells LO2 and THLE-3 and in HCC cell lines (Hep3B, MHCC97L, Huh7, HCCC-9810, HepG2, BEL-7402, MHCC97H, QGY-7703). Transcript levels were normalized to *U6* expression. (**C**) Real-time PCR analysis of miR-105 expression in primary HCC tissues (T) with matched adjacent non-tumor tissues (ANT) from 16 patients. Transcript levels were normalized to *U6* expression. Each bar represents the mean ± SD of three independent experiments. *$P < 0.05$.

anti-α-tubulin monoclonal antibody (Sigma, St Louis, MO) as a loading control. The signals of western blotting bands of Figure 6B were quantified by densitometry, which determined by comparing the ratio in tumor 2 (T2), i.e. the ratio IRS1/α-tubulin, or PDK1/α-tubulin, or Akt1/α-tubulin in T2 was considered as 1.0. The relative expression of miR-105 in tumors was quantified by real-time PCR, which determined by comparing the miR-105 expression in T2 (i.e. the expression of miR-105 was considered as 1.0). The correlation analysis between IRS1/α-tubulin ratio, or PDK1/α-tubulin ratio, or Akt1/α-tubulin ratio with miR-105 expression was performed by Student's two-tailed *t*-test.

3-(4,5-dimethyl-2-thiazolyl)-2,5-diphenyl-2H-tetrazolium bromide assay

Cells were seeded on 96-well plates and stained at indicated time points with 100 µl sterile 3-(4,5-dimethyl-2-thiazolyl)-2,5-diphenyl-2H-tetrazolium bromide dye (0.5 mg/ml, Invitrogen) for 4 h at 37°C, followed by removal of the culture medium and addition of 150 µl of dimethyl sulfoxide (Sigma). The absorbance was measured at 570 nm, with 655 nm as the reference wavelength. All experiments were performed in triplicates.

Colony formation assay

Cells were seeded in a six-well plate (0.5×10^3 cells per well) and cultured for 10 days. Colonies were then fixed with 10% formaldehyde for 10 min and stained for 5 min with 1.0% crystal violet. All experiments were performed in triplicates.

Anchorage-independent growth ability assay

Trypsinized cells (2×10^3) were suspended in 2 ml complete medium plus 0.33% agar (Sigma). The agar-cell mixture was plated as a top layer onto a bottom layer comprising 0.66% complete medium agar mixture. After 10 days culture, colony size was measured using an ocular micrometer and colonies >0.1 mm in diameter were counted. All experiments were performed in triplicates.

Flow cytometry analysis

Cells in a culture dish were harvested by trypsinization, washed in ice-cold phosphate-buffered saline (PBS) and fixed in 80% ice-cold ethanol in PBS. The cells were then pelleted and resuspended in cold PBS. Bovine pancreatic RNAase (2 µg/ml, Sigma) was added and cells were incubated at 37°C for 30 min, followed by incubation in propidium iodide (10 µg/ml, Invitrogen)

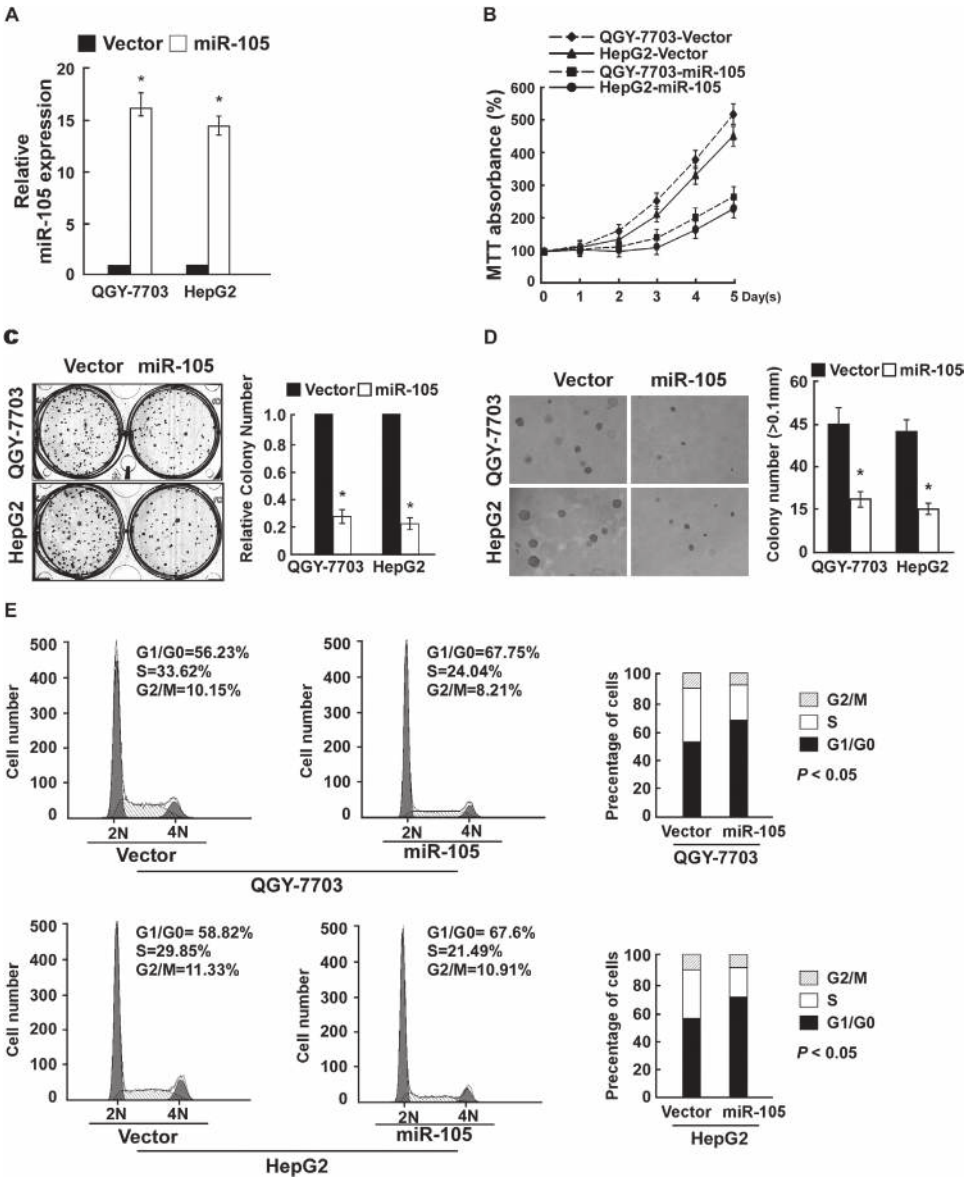

Fig. 2. Ectopic expression of miR-105 inhibited HCC cell proliferation. (**A**) Real-time PCR analysis of miR-105 expression in QGY-7703 and HepG2 cells stably expressing miR-105. (**B**) 3-(4,5-dimethyl-2-thiazolyl)-2,5-diphenyl-2H-tetrazolium bromide assay revealed that miR-105 upregulation suppresses QGY-7703 and HepG2 stable cell lines at indicated times after seeding. (**C**) Representative micrographs (left) and quantification (right) of crystal violet-stained cell colonies. Indicated cells (0.5×10^3) were plated into six-well plates and cultured for 10 days, then stained with crystal violet (1.0%). (**D**) Representative micrographs (left) and quantification of colonies >0.1 mm (right) were scored. Indicated cells (2×10^3) were suspended in soft agar and cultured for 10 days, and then colonies >0.1 mm in diameter were counted. (**E**) Flow cytometry analysis of indicated HCC cells stably expressing miR-105 or vector. Each bar represents the mean ± SD of three independent experiments. *$P < 0.05$.

for 30 min at room temperature. Twenty thousand cells were analyzed by flow cytometry (FACSCalibur, BD Biosciences, San Jose, CA). All experiments were performed in triplicates.

Xenografted tumor model and immunohistochemical

All experimental procedures were approved by the Institutional Animal Care and Use Committee of Sun Yat-Sen University and housed in barrier facilities on a 12 h light/dark cycle. BALB/c nude mice (4–5 weeks of age, 18–20 g) were purchased from the Center of Experimental Animal of Guangzhou University of Chinese Medicine. The BALB/c nude mice were randomly divided into groups (n = 6/group). One group of mice was inoculated subcutaneously with HepG2/vector cells (5×10^6) in the left dorsal flank and with HepG2/miR-105 cells (5×10^6) in the right abdomen flank per mouse. Another two groups were inoculated subcutaneously per mouse with HepG2 cells (5×10^6) in the left abdomen flank. Seven days later, the mice were then intratumorally injected with 100 µl of antagomiR control or antagomiR-105 (diluted in PBS at 2 mg/ml) three times per week for 2 weeks. Tumors were examined twice weekly; length, width and thickness measurements were obtained with calipers and tumor volumes were calculated. Tumor volume was calculated using the equation volume (mm^3) = $(L \times W^2)/2$. On day 37, tumors were detected by an IVIS imagining system (Caliper), then animals were euthanized, tumors were excised, weighed and paraffin embedded. Serial 6.0 µm sections were cut and subjected to immunohistochemical (IHC). After deparaffinization, sections were IHC analyzed using anti-Ki67 (Dako, Glostrup, Denmark) was performed on sections from paraffin-embedded samples for histological evidence of the tumor phenotype. Proliferation index was quantized by counting proportion of Ki67-positive cells.

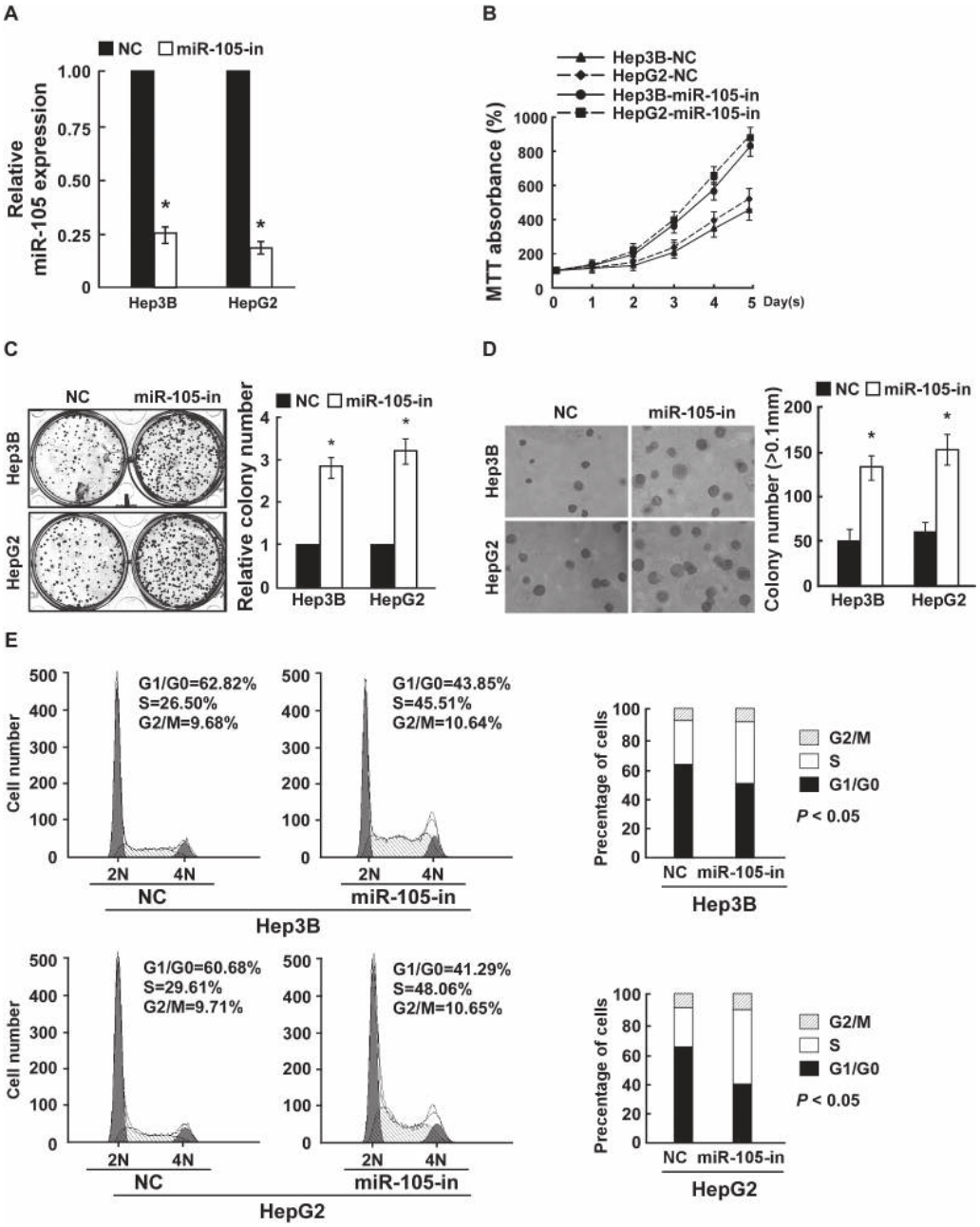

Fig. 3. Inhibiting miR-105 expression enhanced HCC cell proliferation. (**A**) Real-time PCR analysis of miR-105 expression in Hep3B and HepG2 cells transfected with miR-105-in or negative control (NC). (**B**) 3-(4,5-dimethyl-2-thiazolyl)-2,5-diphenyl-2H-tetrazolium bromide analysis of the proliferation ability of HCC cells transfected with miR-105-in or NC. (**C**) Representative micrographs (left) and quantification (right) of HCC cell colonies in indicated HCC cell lines, as determined by colony formation assay. (**D**) Tumorigenicity of HCC cells transfected with miR-105-in or NC was measured by anchorage-independent growth ability assay. Colonies >0.1 mm in diameter were scored. (**E**) Flow cytometry analysis of indicated HCC cells transfected with miR-105-in or NC. Each bar represents the mean ± SD of three independent experiments. *$P < 0.05$.

Statistical analysis

All data were expressed as the mean ± SD. Student's two-tailed *t*-test was used to evaluate the significance of the differences between two groups of data in all the pertinent experiments. The *P* value reported was two sided, and a value of $P < 0.05$ was considered statistically significant.

Results

miR-105 is downregulated in HCC

Using a published microarray-based high-throughput assessment, we found that the expression of miR-105 (Accession: MIMAT0000102) was significantly downregulated in HCC tissues than that in matched non-cancerous liver tissue ($n = 166$; $P < 0.001$; NCBI/GEO/GSE31384; Figure 1A). Furthermore, real-time PCR assay showed that miR-105 expression was markedly lower in all eight HCC cell lines (Hep3B, MHCC97L, Huh7, HCCC-9810, HepG2, BEL-7402, MHCC97H, QGY-7703), compared with that in normal liver epithelial cells LO2 and THLE-3 (Figure 1B). Comparative analysis also revealed that miR-105 was downregulated in the 16 tumor tissue samples compared with adjacent non-cancerous tissues (Figure 1C). Collectively, our results suggest that miR-105 is downregulated in HCC cell lines and tissues.

Ectopic expression of miR-105 inhibited HCC cell proliferation in vitro

To investigate biological role of miR-105 in HCC progression, we established the HCC cell lines QGY-7703 and HepG2 to stably express miR-105 or vector (Figure 2A). The result of 3-(4,5-dimethyl-2-thiazolyl)-2,5-diphenyl-2H-tetrazolium bromide assay showed that overexpression of miR-105 significantly inhibited the growth rate of both HCC cells compared with control cells (Figure 2B). The colony formation assay revealed that miR-105 overexpression resulted in decreased proliferation in both HCC cells (Figure 2C). Additionally, the anchorage-independent growth assay showed the similar results: QGY-7703-miR-105 and HepG2-miR-105 stable cells represented fewer and smaller-sized colonies than the control cells (Figure 2D). We further analyzed the cell cycle of two stable cells by flow cytometry. There was a dramatic increase in the percentage of cells in the G_1/G_0 phase and a decrease in the percentage of cells in the S phase in miR-105-overexpressing cells, compared with that in the control group (Figure 2E). These results suggest that miR-105 upregulation inhibits HCC cell proliferative capacity *in vitro*.

miR-105 inhibition promoted HCC cell proliferation in vitro

To further test whether miR-105 inhibition would promote HCC cell proliferation, we performed loss-of-function studies using a miR-105 inhibitor (miR-105-in), the HCC cell lines Hep3B and HepG2 were selected (Figure 3A). As shown in Figure 3B and C, suppression of miR-105 significantly enhanced the growth rate of both Hep3B and HepG2 cells transfected with the miR-105-in compared with that of negative control transfected cells. The anchorage-independent growth assay revealed that following miR-105-in transfection, both HCC cell lines produced more and larger colonies than the negative control cells (Figure 3D). Moreover, flow cytometry analysis revealed a dramatic decrease in the percentage of cells at G_1/G_0 phase and an increase in the percentage of cells at S phase in miR-105-in transfected cells, compared with that in negative control transfected cells (Figure 3E). Taken together, these results suggest that miR-105 downregulation promotes the proliferation of HCC cells *in vitro*.

miR-105 downregulation contributed to HCC progression in vivo

To investigate whether miR-105 inhibits HCC progression *in vivo*, we used a xenografted tumor model to examine the biological effect of miR-105. As shown in Figure 4A–C, the tumors formed

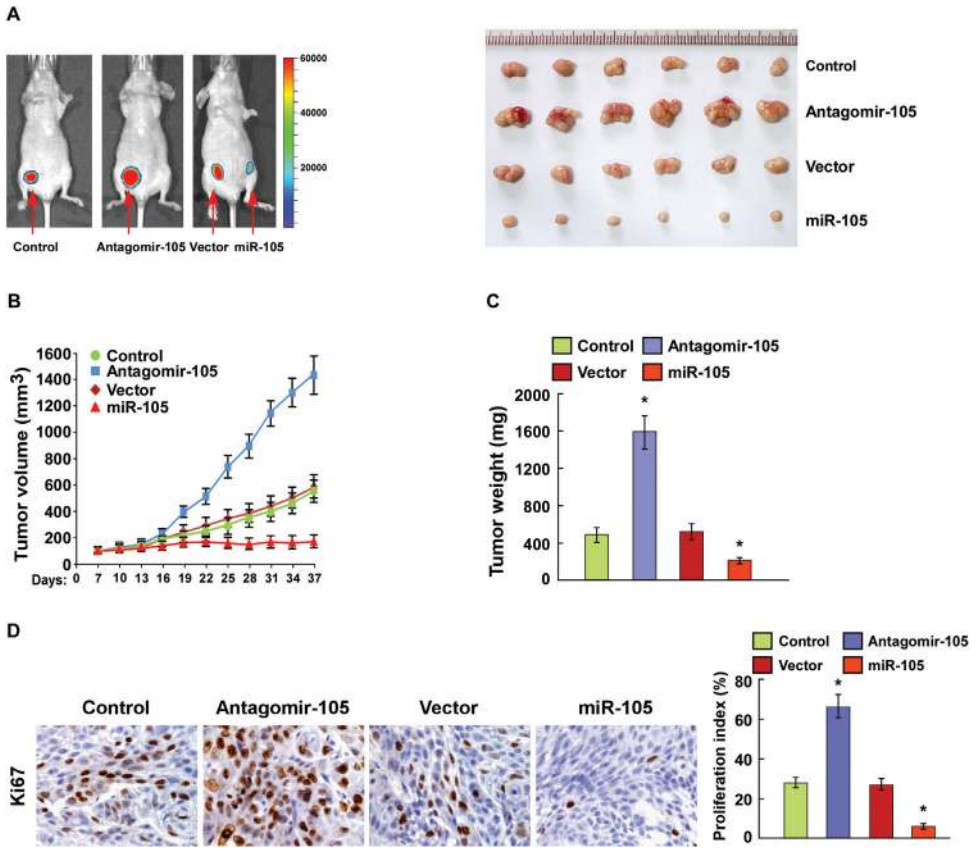

Fig. 4. miR-105 downregulation contributed to HCC progression *in vivo*. (**A**) Representative images of tumor-bearing mice (left) and images of the tumors from all of the mice in each group (right). (**B**) Tumor volumes were measured on the indicated days. (**C**) Mean tumor weights. (**D**) IHC staining showing that miR-105 downregulation increased the percentages of Ki-67 positive cells, whereas miR-105 overexpression inhibited it. Each bar represents the mean ± SD of three independent experiments. *$P < 0.05$.

by miR-105-silenced cells were larger in both size and weight than the tumors formed by control cells. Conversely, the tumors formed by miR-105-transduced HCC cells were smaller and lighter than the control tumors. Furthermore, IHC analysis revealed that miR-105-silenced tumors showed higher percentages of Ki-67-positive cells, whereas miR-105-overexpressing tumors displayed lower Ki-67 proliferation index than the control tumors (Figure 4D). Collectively, these results strongly demonstrate the biological function of miR-105 as a tumor suppressor in HCC *in vivo*.

miR-105 suppressed IRS1, AKT1 and PDK1 directly

To explore the mechanism underlying the growth inhibition by miR-105 in HCC cells, we used publicly available algorithms (TargetScan, miRanda, miRwalk) to predict the potential targets of miR-105 in humans. Three critical components of the PI3K/AKT signal pathway, including IRS1, PDK1 and AKT1, were predicated as potential targets of miR-105 by the all three algorithms (Figure 5A). Western blotting showed that IRS1, PDK1 and AKT1 expression in both QGY-7703 and HepG2 cells were dramatically downregulated in response to miR-105 transfection and was upregulated by miR-105-in (Figure 5B). To further confirm whether IRS1, PDK1 and AKT1 are direct targets of miR-105, we performed the luciferase reporter assay. As shown in Figure 5C, ectopic expression of miR-105 decreased the luciferase activity of the 3′UTRs of IRS1, PDK1 and AKT1 and miR-105-in increased it. However, miR-105 mutant containing three altered nucleotides in the seed sequence did not have an inhibitory effect on luciferase activity.

miR-105 overexpression inhibited the PI3K/AKT signaling pathway

As the above-mentioned miR-105 targets are closely correlated with PI3K/AKT signaling, we then further examined the effect of miR-105 deregulation on the expression of downstream genes of the PI3K/AKT signaling pathway. Figure 5D illustrates the dramatic increase in the expression of phosphorylated FOXO3a (pFOXO3a), the direct target of AKT kinase, in miR-105-overexpressing cells; pFOXO3a was decreased in cells transfected with miR-105-in. The expression of p21 and p27, the downstream genes regulated by FOXO3a, was dramatically increased in miR-105-overexpressing cells, whereas miR-105-in transfection decreased their expression at both messenger RNA and protein level (Figure 5D and Supplementary Figure 1, available at *Carginogenesis* online). Consistently, the expression of Cyclin D1, another FOXO3a downstream gene, was downregulated following miR-105 overexpression

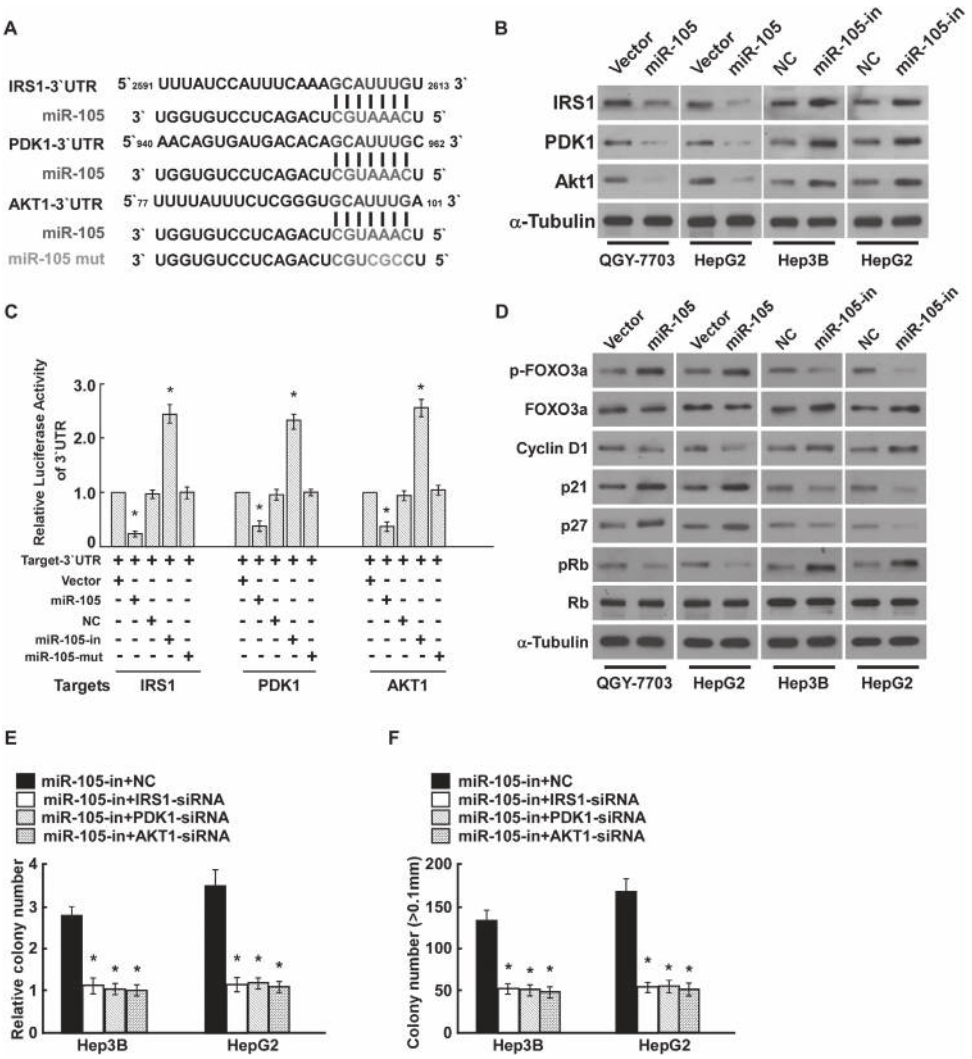

Fig. 5. IRS1, PDK1 and AKT1 are direct targets of miR-105. (**A**) Predicted miR-105 target sequences in the 3′UTRs of IRS1, PDK1 and AKT1. The miR-105 mutant (miR-105-mut) contained three altered nucleotides in the seed sequence. (**B**) Western blotting analysis of IRS1, PDK1 and AKT1 expression in the indicated HCC cells. α-Tubulin served as loading control. (**C**) Luciferase assay of pGL3-*IRS1*-3′UTR, pGL3-*PDK1*-3′UTR and pGL3-*AKT1*-3′UTR reporter cotransfected with miR-105 mimic, miR-105- inhibitor and miR-105-mut oligonucleotides in HCC cells. (**D**) Western blotting analysis of p-FOXO3a, FOXO3a, Cyclin D1, p21, p27, Rb and p-Rb expression in HCC cells. α-Tubulin served as the loading control. (**E**) Quantification of crystal violet-stained HCC cell colonies formed, 10 days after inoculation. (**F**) Quantification of colony numbers as determined by anchorage-independent growth assay. Colonies >0.1 mm in diameter were scored. Each bar represents the mean ± SD of three independent experiments. *$P < 0.05$.

and upregulated by miR-105 suppression (Figure 5D and Supplementary Figure 1, available at *Carginogenesis* online). As expected, miR-105 overexpression decreased the level of phosphorylated retinoblastoma protein, but inhibiting miR-105 increased phosphorylated retinoblastoma protein (Figure 5D). Taken together, our results suggest that miR-105 overexpression inhibits the P3K/AKT signaling pathway.

To examine the effect of IRS1, AKT1 or PDK1 suppression on the proliferative capacity of miR-105-in cells in HCC, we suppressed endogenous expression of these three targets using RNA interference. As shown in Figure 5E and F and Supplementary Figure 2A–C, available at *Carcinogenesis* online, individual silencing of these target genes decreased cell growth rate and proliferation potently, as assessed by colony formation assay and anchorage-independent growth assay, respectively. These results suggest that IRS1, PDK1 and AKT1 are essential for miR-105 downregulation-mediated HCC cell proliferation.

Clinical relevance of miR-105 level and IRS1, AKT1 and PDK1 expression in HCC

To examine the clinical relationship between miR-105 and its targets, we examined miR-105 levels and the expression of IRS1, AKT1 or PDK1 in eight fresh clinical HCC tissue samples (Figure 6A). Statistical analysis demonstrated that miR-105 expression was inversely correlated with IRS1 ($r = -0.742$, $P = 0.031$), PDK1 ($r = -0.827$, $P = 0.040$), AKT1 expression ($r = -0.745$, $P = 0.035$) (Figure 6B), supporting the notion that miR-105 downregulation promotes proliferation in HCC and activates the PI3K/AKT signaling pathway by directly suppressing IRS1, AKT1 or PDK1.

Discussion

Our study presents the important finding that miR-105 expression is markedly downregulated in both HCC cells and clinical tissues. Ectopic expression of miR-105 robustly attenuated, whereas suppression of endogenous miR-105 promoted the proliferation and tumorigenicity of HCC cells *in vitro* and *in vivo*. Furthermore, we demonstrated that ectopic miR-105 expression in HCC cells inhibited the PI3K/AKT pathway activity through directly repressing IRS1, PDK1 and AKT1, which were further confirmed in the clinical HCC samples. These findings suggest that miR-105 might play an important role in HCC progression by controlling PI3K/AKT signaling.

miRNA dysregulation frequently occurs in various human tumors, and aberrant miRNA expression contributes to human carcinogenesis by affecting the expression of multiple genes (22). Therefore, a comprehensive understanding of the relationship between specific miRNAs and tumor development is valuable for tumor diagnosis and therapy. It should be noted that miR-105 is downregulated or upregulated in different tumor types. For example, miR-105 has been found to downregulated in human tumors, such as prostate cancer and miR-105 downregulation contributes to prostate tumor cell proliferation both *in vitro* and *in vivo* (23). Meanwhile, through assessment of a published microarray, we also found that the expression of miR-105 was significantly downregulated in colon cancer tissues than that in matched non-cancerous colon tissue ($n = 226$; TCGA data set/COAD). To investigate the biological functions and underlying molecular mechanism of miR-105 in HCC development, we examined miR-105 expression in HCC and found that it was downregulated in HCC. Meanwhile, miR-105 upregulation dramatically repressed the proliferation of HCC cells and inhibited PI3K/AKT signaling, which further demonstrated the tumor-suppressive role of miR-105 in HCC. Concordant with that of previous studies, our findings indicate an important role of miR-105 in modulating tumor progression and it may represent a promising therapeutic target in HCC. However, a comprehensive miRNA-profiling study of colorectal cancer showed that miR-105 was upregulated in tumor tissues compared with normal mucosa (24). Recently, Zhou *et al.* (25) reported that overexpression of miR-105 in non-metastatic cancer cells induces metastasis and vascular permeability in distant organs, whereas inhibition of miR-105 in highly metastatic tumors alleviates these effects, which suggests that miR-105 might present as a potent regulator of breast cancer migration. Collectively, these findings suggest that the miR-105 expression and its biological functions might be tumor-type dependent. Therefore, the clinical significance and mechanism of miR-105 downregulation in HCC require further investigation.

Aberrant PI3K/AKT signaling pathway activation is found in a wide spectrum of human tumors, including HCC, significantly contributing to the formation and progression of these malignancies (26). Strikingly, the three *bona fide* target genes of miR-105 identified in our study, namely IRS1, PDK1 and AKT1, are overexpressed in multiple tumors and are essential for specific and effective activation of the oncogenic AKT signaling. IRS1 is constitutively activated in human tumors, for instance, breast cancer and human HCC, and plays

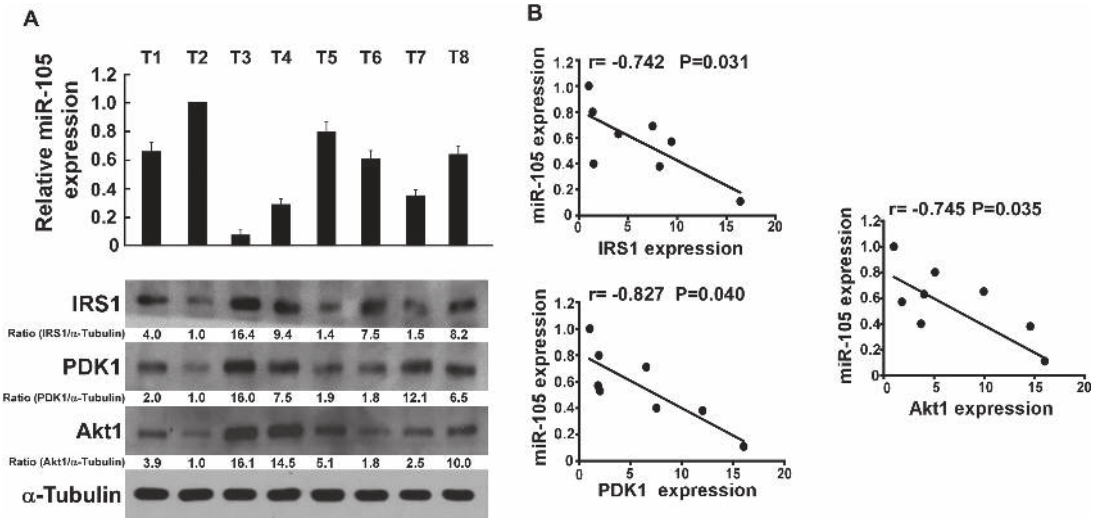

Fig. 6. Clinical relevance of miR-105 downregulation and IRS1, AKT1 and PDK1 in HCC. (**A**) Expression of miR-105 and IRS1, PDK1 and AKT1 protein in another eight clinical HCC tissue samples, as measured by real-time PCR (top) and western blotting (bottom), respectively. α-Tubulin served as loading control. (**B**) Correlation between miR-105 and IRS1, PDK1 and AKT1 expression was analyzed. The relative expression of miR-105 in tumors was quantified by real-time PCR, which determined by comparing the miR-105 expression in T2 (i.e. the expression of miR-105 was considered as 1.0). The correlation analysis between IRS1/α-tubulin ratio, or PDK1/α-tubulin ratio, or Akt1/α-tubulin ratio with miR-105 expression was performed by Student's two-tailed *t*-test. Error bars represent the mean ± SD from of three independent experiments. $^*P < 0.05$.

an important role in tumor development (27,28). IRS1 overexpression occurs as an early event in hepatocarcinogenesis and promotes HCC cell proliferation and invasion (29,30). Sun *et al.* (31) also reported that IRS1 has transformation potential and ectopic expression of IRS1 conferred breast cancer BT-20 cell proliferative ability, for instance, forming colonies in soft agar and tumors in mice. Abnormal PDK1 expression and activity are linked to human disease, including cancer (17). PDK1 is overexpressed in breast carcinomas and is required for anchorage-independent and xenograft growth of breast cancer cells, suggesting that PDK1 inhibition suppresses breast cancer progression (32). AKT1/protein kinase B α is the most extensively studied member of the serine/threonine protein kinase subfamily and is usually referred as AKT. It is well established that extracellular and intracellular stimuli activate AKT1 regulation of tumor cell growth, proliferation, survival, differentiation and metabolism (33). Mei *et al.* (34) reported that AKT1 kinase activity is frequently increased in prostate, breast cancers and ovarian carcinomas, and its constitutive activation is required for oncogenic transformation in mouse NIH3T3 cells. Therefore, it is very likely that IRS1, PDK1 and AKT1 might cooperate act to activate and promote tumor progression, and suppressing the three genes simultaneously might represent an efficient strategy for suppressing oncogenesis. Herein, we demonstrate that miR-105 suppresses IRS1, PDK1 and AKT1 expression by directly targeting their 3′UTRs. Consistent with the oncogenic effects of IRS1, PDK1 and AKT1 in HCC, miR-105 was downregulated in HCC, and its suppression dramatically promoted HCC cell proliferation both *in vitro* and *in vivo*. Taken together, our results represent a novel mechanism of IRS1, PDK1 and AKT1 upregulation in HCC and a functionally and clinically relevant epigenetic mechanism of HCC pathogenesis.

In conclusion, our current study demonstrates the tumor-suppressive effect of miR-105 in HCC. miR-105 upregulation drastically reduces HCC cell proliferation by inhibiting the expression of three key regulators of the PI3K/AKT signaling pathway, i.e. IRS1, PDK1 and AKT1. These findings improve our understanding of HCC progression and might provide a novel putative target for HCC diagnosis and therapy.

Supplementary material

Supplementary Figures 1–4 can be found at http://carcin.oxfordjournals.org/

Funding

National Science Foundation of China (81101317); Science and Technology Planning Project of Guangdong Province, China (2012B010200027); The Science and Technology Department of Guangzhou (2014J4100063).

Conflict of Interest Statement: None declared.

References

1. Jemal,A. *et al.* (2011) Global cancer statistics. *CA Cancer J. Clin.*, **61**, 69–90.
2. Kudo,M. (2011) Hepatocellular carcinoma in 2011 and beyond: from the pathogenesis to molecular targeted therapy. *Oncology*, **81**(suppl. 1), 1–10.
3. Meguro,M. *et al.* (2011) The molecular pathogenesis and clinical implications of hepatocellular carcinoma. *Int. J. Hepatol.*, **2011**, 818672.
4. Parkin,D.M. *et al.* (2001) Estimating the world cancer burden: Globocan 2000. *Int. J. Cancer*, **94**, 153–156.
5. Perz,J.F. *et al.* (2006) The contributions of hepatitis B virus and hepatitis C virus infections to cirrhosis and primary liver cancer worldwide. *J. Hepatol.*, **45**, 529–538.
6. Bosch,F.X. *et al.* (2004) Primary liver cancer: worldwide incidence and trends. *Gastroenterology*, **127**, S5–S16.
7. Altomare,D.A. *et al.* (2005) Perturbations of the AKT signaling pathway in human cancer. *Oncogene*, **24**, 7455–7464.
8. Bellacosa,A. *et al.* (2005) Activation of AKT kinases in cancer: implications for therapeutic targeting. *Adv. Cancer Res.*, **94**, 29–86.
9. Chen,K.F. *et al.* (2011) Activation of phosphatidylinositol 3-kinase/Akt signaling pathway mediates acquired resistance to sorafenib in hepatocellular carcinoma cells. *J. Pharmacol. Exp. Ther.*, **337**, 155–161.
10. Zhou,Q. *et al.* (2011) Targeting the PI3K/Akt/mTOR pathway in hepatocellular carcinoma. *Future Oncol.*, **7**, 1149–1167.
11. Maehama,T. *et al.* (1998) The tumor suppressor, PTEN/MMAC1, dephosphorylates the lipid second messenger, phosphatidylinositol 3,4,5-trisphosphate. *J. Biol. Chem.*, **273**, 13375–13378.
12. Ivetac,I. *et al.* (2005) The type Ialpha inositol polyphosphate 4-phosphatase generates and terminates phosphoinositide 3-kinase signals on endosomes and the plasma membrane. *Mol. Biol. Cell*, **16**, 2218–2233.
13. Brognard,J. *et al.* (2007) PHLPP and a second isoform, PHLPP2, differentially attenuate the amplitude of Akt signaling by regulating distinct Akt isoforms. *Mol. Cell*, **25**, 917–931.
14. Wilden,P.A. *et al.* (1996) Insulin receptor structural requirements for the formation of a ternary complex with IRS-1 and PI 3-kinase. *Mol. Cell. Endocrinol.*, **122**, 131–140.
15. Kuhné,M.R. *et al.* (1993) The insulin receptor substrate 1 associates with the SH2-containing phosphotyrosine phosphatase Syp. *J. Biol. Chem.*, **268**, 11479–11481.
16. Mohr,L. *et al.* (1998) Ethanol inhibits hepatocyte proliferation in insulin receptor substrate 1 transgenic mice. *Gastroenterology*, **115**, 1558–1565.
17. Carnero,A. (2010) The PKB/AKT pathway in cancer. *Curr. Pharm. Des.*, **16**, 34–44.
18. Potente,M. *et al.* (2005) Involvement of Foxo transcription factors in angiogenesis and postnatal neovascularization. *J. Clin. Invest.*, **115**, 2382–2392.
19. Dansen,T.B. *et al.* (2008) Unravelling the tumor-suppressive functions of FOXO proteins. *Trends Cell Biol.*, **18**, 421–429.
20. Ambros,V. (2004) The functions of animal microRNAs. *Nature*, **431**, 350–355.
21. Bartel,D.P. (2004) MicroRNAs: genomics, biogenesis, mechanism, and function. *Cell*, **116**, 281–297.
22. Kloosterman,W.P. *et al.* (2006) The diverse functions of microRNAs in animal development and disease. *Dev. Cell*, **11**, 441–450.
23. Honeywell,D.R. *et al.* (2013) miR-105 inhibits prostate tumour growth by suppressing CDK6 levels. *PLoS One*, **8**, e70515.
24. Hamfjord,J. *et al.* (2012) Differential expression of miRNAs in colorectal cancer: comparison of paired tumor tissue and adjacent normal mucosa using high-throughput sequencing. *PLoS One*, **7**, e34150.
25. Zhou,W. *et al.* (2014) Cancer-secreted miR-105 destroys vascular endothelial barriers to promote metastasis. *Cancer Cell*, **25**, 501–515.
26. Testa,J.R. *et al.* (2005) AKT signaling in normal and malignant cells. *Oncogene*, **24**, 7391–7393.
27. Chang,Q. *et al.* (2002) Constitutive activation of insulin receptor substrate 1 is a frequent event in human tumors: therapeutic implications. *Cancer Res.*, **62**, 6035–6038.
28. Belfiore,A. *et al.* (1996) Insulin receptors in breast cancer. *Ann. N. Y. Acad. Sci.*, **784**, 173–188.
29. Taouis,M. *et al.* (1998) Insulin receptor substrate 1 antisense expression in an hepatoma cell line reduces cell proliferation and induces overexpression of the Src homology 2 domain and collagen protein (SHC). *Mol. Cell. Endocrinol.*, **137**, 177–186.
30. Nishiyama,M. *et al.* (1992) Cloning and increased expression of an insulin receptor substrate-1-like gene in human hepatocellular carcinoma. *Biochem. Biophys. Res. Commun.*, **183**, 280–285.
31. Sun,H. *et al.* (2008) The role of insulin receptor substrate-1 in transformation by v-src. *J. Cell. Physiol.*, **215**, 725–732.
32. Gagliardi,P.A. *et al.* (2012) 3-phosphoinositide-dependent kinase 1 controls breast tumor growth in a kinase-dependent but Akt-independent manner. *Neoplasia*, **14**, 719–731.
33. Nicholson,K.M. *et al.* (2002) The protein kinase B/Akt signalling pathway in human malignancy. *Cell Signal*, **14**, 381–395.
34. Mei Sun,G.W. *et al.* (2001) AKT1PKBα Kinase is frequently elevated in human cancers and its constitutive activation is required for oncogenic transformation in NIH3T3 cells. *Am. J. Pathol.*, **159**, 431–437.

Received June 2, 2014; revised August 22, 2014; accepted September 21, 2014